Signal Processing:
An International Journal (SPIJ)

Table of Contents

Volume 3, Issue 2, April 2009.

Pages

Mohamed Nerma, Nidal Kamel, and Varun Jeoti

An OFDM System Based on Dual Tree Complex Wavelet Transform (DT-CWT)

Mohamed H. M. Nerma   mohamed_hussien@ieee.org
Electrical and Electronic Engineering Department
University Technology PETRONAS
Bandar Seri Iskandar, Tronho, 31750 Perak, Malaysia

Nidal S. Kamel   nidalkamel@petronas.com.my
Electrical and Electronic Engineering Department
University Technology PETRONAS
Bandar Seri Iskandar, Tronho, 31750 Perak, Malaysia

Varun Jeoti   varun_jeoti@petronas.com.my
Electrical and Electronic Engineering Department
University Technology PETRONAS
Bandar Seri Iskandar, Tronho, 31750 Perak, Malaysia

ABSTRACT

In this paper, a novel orthogonal frequency division multiplexing (OFDM) system based on dual–tree complex wavelet transform (DT-CWT), is presented. In the proposed system, the DT-CWT is used to replace the fast Fourier transform (FFT) in the conventional OFDM. This results in considerable improvement in terms of bit error rate (BER) over not only the conventional OFDM but also to the wavelet packet modulation (WPM) based OFDM system. Moreover, the proposed system achieves better peak–to–average power ratio (PAPR) performance at acceptable increase in computational complexity. The complementary cumulative distribution function of PAPR for the proposed system shows ≈ 3 dB improvement over the conventional and the WPM based OFDM systems.

Keywords: OFDM, WPT, DT-CWT, FFT, Multicarrier Modulation.

1. INTRODUCTION

Traditionally, orthogonal frequency division multiplexing (OFDM) is implemented using fast Fourier transform (FFT). However, FFT has a major drawback arising from using rectangular window, which creates sidelobes. Moreover, the pulse shaping function used to modulate each subcarrier extends to infinity in the frequency domain. This leads to high interference and lower performance levels. Intercarrier interference (ICI) and intersymbol interference (ISI) can be avoided by adding a cyclic prefix (CP) to the head of OFDM symbol. But, this reduces the spectrum efficiency.

The wavelet packet modulation (WPM) system has a higher spectral efficiency and better robustness towards inter-channel interference than the conventional OFDM system. Moreover, WPM is capable of decomposing the time frequency plane in flexible way through filter bank (FB) constructions [1].

Mohamed Nerma, Nidal Kamel, and Varun Jeoti

WPM system does not require CP, and according to the IEEE broadband wireless standard IEEE 802.16.3, avoiding CP gives wavelet OFDM an advantage of roughly 20% in bandwidth efficiency. Moreover, pilot tones are not needed with WPM system. This gives wavelet based OFDM system another 8% advantage over typical OFDM implementations [2].

However, the major problem with the common discrete wavelet packet transform (DWPT) is its lack of shift invariance; which means that on shifts of the input signal, the wavelet coefficients vary substantially. The signal information may not be stationary in the sub-bands so that the energy distribution across the sub-bands may change [3]. To overcome the problem of shift dependence, one possible approach is to simply omit the sub-sampling causing the shift dependence. Techniques that omit or partially omit sub-sampling are cycle spinning, oversampled FBs or undecimated wavelet transform (UWT). However, these transforms are redundant [4], which is not desirable in multicarrier modulation, as the complexity of redundant transform is high. In this paper we propose an OFDM system based on dual-tree complex wavelet transform (DT-CWT). This system is non-redundant achieves approximate shift invariance and is also inherits all the advantages of WPM system [5].

This paper is organized as follows: In section 2, we discuss the dual-tree complex wavelet transform (DT-CWT); in section 3, the multicarrier modulation systems (MCM) are discussed; the simulation results are presented in section 4; and we conclude this paper in section 5.

2. The Dual Tree Complex Wavelet Transform (DT-CWT)

Since early 1990s the WT and WPT have been receiving an increased attention in modern wireless communications [6]. A number of modulation schemes based on wavelets have been proposed [7], [8], - [15]. The DT-CWT was introduced by Kingsbury [16] – [20] as two real discrete WT (DWT). The upper part of the FB gives the real part of the transform while the lower one gives the imaginary part. This transform uses the pair of the filters ($h_0(n)$, $h_1(n)$ the low-pass/high-pass filter pair for the upper FB respectively) and ($g_0(n)$, $g_1(n)$ the low-pass/high-pass filter pair for the lower FB respectively) that are used to define the sequence of wavelet function $\psi_h(n)$, $\frac{}{g}$ and scaling function $\phi_h(n)$, $\frac{}{g}$ as follows

$$\psi_h(t) = \sqrt{2} \sum_n h_1(n)\phi_h(2t - n) \qquad\qquad 1$$

$$\phi_h(t) = \sqrt{2} \sum_n h_0(n)\phi_h(2t - n) \qquad\qquad 2$$

where $h_1(n) = (-1)^n h_0(d - n)$. The wavelet function $\psi_g(t)$, the scaling function $\phi_g(t)$ and the high-pass filter for the imaginary part $g_1(n)$ are defined in similar way. The two real wavelets associated with each of the two real transform are $\psi_h(t)$ and $\psi_g(t)$. To satisfy the perfect reconstruction (PR) conditions, the filters are designed so that the complex wavelet $\psi(t) = \psi_h(t) + j\psi_g(t)$ is approximately analytic. Equivalently, they are designed so that $\psi_g(t)$ is approximately the Hilbert transform of $\psi_h(t)$.

$$\psi_g(t) = H\{\psi_h(t)\} \qquad\qquad 3$$

The analysis (decomposition or demodulation) and the synthesis (reconstruction or modulation) FBs used to implement the DT-CWT and their inverses are illustrated in fig. 1 and fig. 2 respectively. The inverse of DT-CWT is as simple as the forward transform. To invert the transform, the real and the imaginary parts are inverted.

Mohamed Nerma, Nidal Kamel, and Varun Jeoti
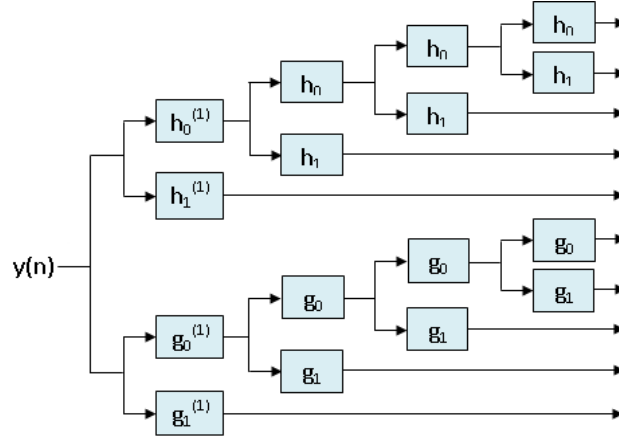
**FIGURE 1:** The dual tree discrete CWT (DT-DCWT) Analysis (demodulation) FB.
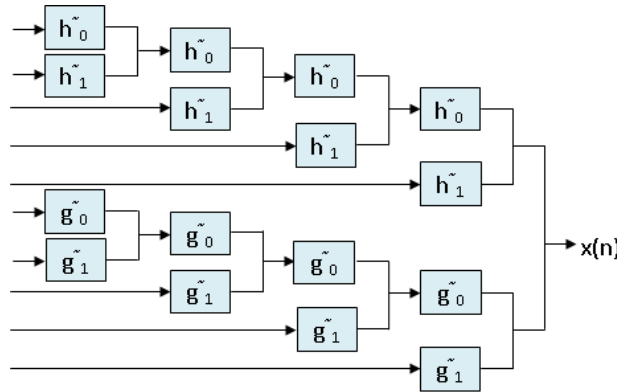
FIGURE 2: The Inverse dual tree discrete CWT (IDT-DCWT) Synthesis (modulation) FB.

The two low pass filters should satisfy the condition of one of them being approximately a half-sample shift of the other [21]

$$g_0(n) \approx h_0(n - 0.5) \Rightarrow \psi_g(t) \approx H\{\psi_h(t)\} \qquad 4$$

Since $g_0(n)$ and $h_0(n)$ are defined only on the integers, this statement is somewhat informal. However, we can make the statement rigorous using FT. In [4] it is shown that, if $G_0(e^{j\omega}) = e^{-j0.5\omega} H_0(e^{j\omega})$, then $\psi_g(t) = H\{\psi_h(t)\}$. The converse has been proven in [22] [23], making the condition necessary and sufficient. The necessary and sufficient conditions for biorthogonal case were proven in [24]. The half-sample delay condition given in terms of magnitude and phase function is given as

$$\left| G_0(e^{j\omega}) \right| = \left| H_0(e^{j\omega}) \right| \qquad 5$$

$$\angle(e^{j\omega}) = \angle H_0(e^{j\omega}) - 0.5\omega \qquad 6$$

In practical implementation of the DT-CWT, the delay condition (5) and (6) are approximately satisfied and the wavelets $\psi_h(t)$ and $\psi_g(t)$ are approximately Hilbert pairs, thus the complex wavelet $\psi_h(t) + j\psi_g(t)$ are approximately analytic. On the other hand, the FT is based on a complex valued oscillating cosine and sine components that form complete Hilbert transform

pairs; i.e., they are 90° out of phase of each other. Together they constitute an analytic signal, $e^{j\theta t}$, that is supported on one-half of the frequency axis $(\theta > 0)$ [16].

3. DT-CWT Based OFDM

In the baseband equivalent conventional OFDM transmitter with m^{th} frame of N QAM or PSK symbols, a_k^m , $k = 0,1,...,N-1,$ the OFDM frame is given by:

$$x^m[n] = \sum_{k=0}^{N-1} a_k^m e^{\frac{j2\pi nk}{N}}$$ 7

for AWGN channel. The received signal is given as

$$y(n) = \propto x(n) + w(n),$$ 8

where $\propto$ is the attenuation factor per block of data and $w(n)$ is the AWGN noise. At receiver side the transmitted data is recovered.

$$\hat{a}_l^m = \langle y(n), e^{\frac{-j2\pi nl}{N}} \rangle - \langle w(n), e^{\frac{j2\pi nl}{N}} \rangle,$$ 9

With WPM system [4], the transmitted signal $x[n]$ is constructed as the sum of M wavelet packet function $\phi_j[n]$ individually modulated with the QAM or PSK symbols.

$$x[n] = \sum_i \sum_{j=0}^{M-1} a_{i,j} \phi_j[n-iM]$$ 10

And at receiver side, the transmitted data is recovered from the received signal $y(n)$.

$$\hat{a}_{i,j} = \langle y(n), \phi_j[n-iM] \rangle - \langle w(n), \phi_j[n-iM] \rangle,$$ 11

Similar to the conventional OFDM and WPM systems, a functional block diagram of OFDM based on DT-CWT is shown in fig. (3). At the transmitter an inverse DT-CWT (IDT-CWT) block is used in place of inverse FFT (IFFT) block in conventional OFDM system or in place of the inverse DWPT (IDWPT) block in WPM system. At the receiver side a DT-CWT is used in place of FFT block in conventional OFDM system or in place of DWPT block in WPM system.
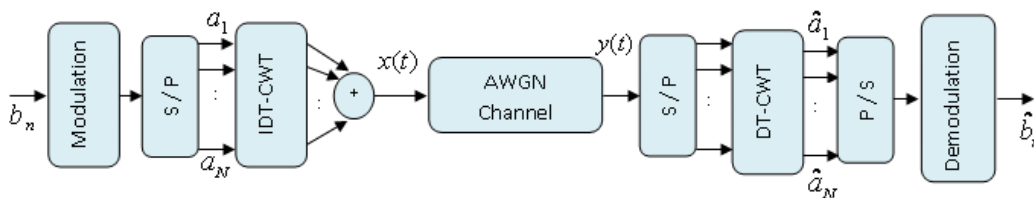

FIGURE 3: DT-CWT modulation (DT-CWTM) functional block diagram.

Data to be transmitted is typically in the form of a serial data stream. PSK or QAM modulations can be implemented in the proposed system and the choice depends on various factors, like the

Mohamed Nerma, Nidal Kamel, and Varun Jeoti

bit rate and sensitivity to errors. The transmitter accepts modulated data (in this paper we use 16 and 64QAM). At transmitter, the data stream is first passed through a serial to parallel (S/P) converter, giving N lower bit rate data streams. The data is then modulated using an IDT-CWT matrix realized by an N-band synthesis FB.

IDT-CWT works in a similar fashion to an IFFT or IDWPT. It takes as the input QAM symbols and outputs them in parallel time-frequency "subcarriers". In fig. (2) as the synthesis process, it can be shown that the transmitted signal, $x[n]$ can be written as follows:

Let $\varphi(n)$ be the scaling function, $\psi(n)$ be the wavelet function, and a_i is k^{th} symbol, $i = 1, 2, ..., N$

$$x(n) = R_e\,[x(n)] + jI_m\,[x(n)].\qquad\qquad 12$$

$$R_e\,[x(n)] = a_{1,k}\,\varphi_{1,k}(n) + \sum_{j=2}^{\frac{N}{2}} a_{j,k}\,\psi_{j,k}(n).\qquad\qquad 13$$

$$I_m\,[x(n)] = a_{\frac{N}{2}+1,k}\,\varphi_{\frac{N}{2}+1,k}(n) + \sum_{j=\frac{N}{2}+2}^{N} a_{j,k}\,\psi_{j,k}(n).\qquad\qquad 14$$

The received signal can be written in the following form:

$$y(n) = a_{1,k}\,\hat{\varphi}_{1,k}(n) + \sum_{j=2}^{\frac{N}{2}} a_{j,k}\,\hat{\psi}_{j,k}(n) + j\left(a_{\frac{N}{2}+1,k}\,\hat{\varphi}_{\frac{N}{2}+1,k}(n) + \sum_{j=\frac{N}{2}+2}^{N} a_{j,k}\,\hat{\psi}_{j,k}(n)\right) + w(n).\qquad 15$$

where $\hat{\varphi}_{m,n}(n) = \propto \varphi_{m,n}(n)$ and $\hat{\psi}_{m,n}(n) = \propto \psi_{m,n}(n)$.

$$\langle y(n), [\varphi]_1(1,k)(n)\rangle = a_1(1,k)\,\langle[\varphi]_1(1,k)(n), [\varphi]_1(1,k)(n)\rangle + \Sigma_1(j=2)^{T}(N/2)\,[a_1(j,k)\,([\psi]_1(j,$$

For perfect synchronization and orthogonality between subcarrier, to recover the transmitted data in each symbol we match the transmitted waveform with the carrier j according to the following formula:

$$\langle \varphi_{j,k}(n), \varphi_{m,n}(n)\rangle = \langle \psi_{j,k}(n), \psi_{m,n}(n)\rangle = \begin{cases} 1, & if\ j = m\ \ and\ \ k = n \\ 0, & otherwise \end{cases}.\qquad 17$$

and

$$\langle \psi_{j,k}(n), \varphi_{m,n}(n)\rangle = 0\qquad\qquad 18$$

Equation (17), (18) indicate that the wavelet function and scaling function are orthogonal to each other, thus we will be able to separate the subcarriers at receiver. Thus,

$$\hat{a}_{1,k} = \langle y(n), \varphi_{1,k}(n)\rangle - \langle w(n), \varphi_{1,k}(n)\rangle.\qquad\qquad 19$$

$$\hat{a}_{\frac{N}{2}+1,k} = \langle y(n), \varphi_{\frac{N}{2}+1,k}(n)\rangle - \langle w(n), \varphi_{\frac{N}{2}+1,k}(n)\rangle.\qquad\qquad 20$$

$$\hat{a}_{j,k}\Big|_{j=1-\frac{N}{2}} = \langle y(n), \psi_{j,k}(n)\rangle - \langle w(n), \psi_{j,k}(n)\rangle\qquad\qquad 21$$

Mohamed Nerma, Nidal Kamel, and Varun Jeoti

$$\hat{d}_{j,k}\Big|_{j=\frac{N}{2}-2\,-N} = \langle y(n),\ \psi_{j,k}(n)\rangle - \langle w(n),\ \psi_{j,k}(n)\rangle \qquad\qquad \mathbf{22}$$

4. Results and Analysis

In this section we show the results for BER, PAPR and PSD respectively. The simulation parameters are documented as follows: Modulation type is 16-QAM and 64 QAM; the number of subcarriers is 64, 128, 256, 512, and 1024 subcarriers; a wavelet packet base is Daubechies-1 (DAUB-1); maximum tree depth (D = 7); PAPR threshold is 2dB; shaping filter is Raised Cosine (rolloff factor $\alpha = 0.001$, upsampler = 4); DT-CWT using different filters (LeGall 5,3 tap filters (leg), Antonini 9,7 tap filters (anto), Near Symmetric 5,7 tap filters (n-sym-a), and Near Symmetric 13,19 tap filters (n-sym-b)) for the first stage of the FB and (Quarter Sample Shift Orthogonal 10,10 tap filters (q-sh-06) only 6,6 non-zero taps, Quarter Sample Shift Orthogonal 10,10 tap filters (q-sh-a) with 10,10 non-zero taps, unlike q-sh-06, Quarter Sample Shift Orthogonal 14,14 tap filters (q-sh-b), Quarter Sample Shift Orthogonal 16,16 tap filters (q-sh-c), and Quarter Sample Shift Orthogonal 18,18 tap filters (q-sh-d)) for the succeeding stages of the FB.

In the first experiment, the BER performance of the DT-CWT-based OFDM system is tested and compared with the conventional OFDM and WPM systems. The Daubechies-1 wavelet packet bases are used to construct the wavelet packet trees in WPM system with maximum tree depth (D = 7). PAPR threshold is 2dB, shaping filter is Raised Cosine (rolloff factor $\alpha = 0.001$, upsampler = 4). 16 QAM and 64 QAM are used with 64 subcarriers. The results are shown in Figure (4).
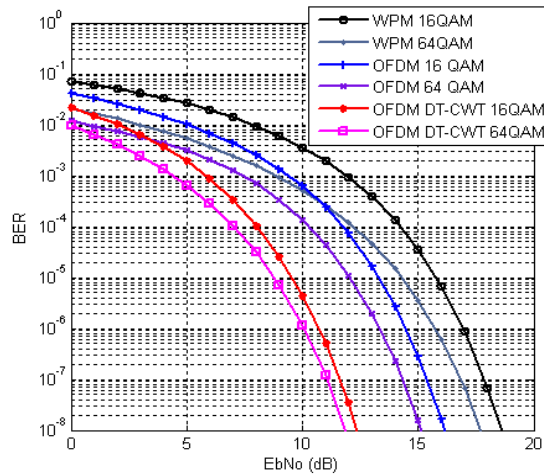

Figure 4: BER performance of OFDM based on DT-CWT using 16 QAM and 64 QAM.

It is quite clear from Fig. (4) that the proposed scheme is significantly outperforming the conventional OFDM and the WPM systems, in term of BER. It is also clear that the conventional OFDM is performing better than the WPM .

The above experiment is repeated for different set of filters. OFDM DT-CWT$_1$ represents the system when using near-symmetric (n-sym) 13,19 tap filters in the first stage of the FB and quarter sample shift orthogonal (q-sh) 14 tap filters in the succeeding stages. OFDM DT-CWT$_2$ represents the system when using (n-sym 13,19 with q-sh 10 (10 non zero taps) filters). OFDM DT-CWT$_3$ is the system when using (antonini (anto) 9,7 tap filters with q-sh0 10 (only 6 non zero taps) filters). OFDM DT-CWT$_4$ is the system when using (anto 9,7 with q-sh 14 filters). OFDM DT-CWT$_5$ is the system when using (n-sym 5,7 with q-sh 14 filters). OFDM DT-CWT_6 is the system

when using (LeGall (leg) 5,3 tap filters with q-sh 14 filters). OFDM DT-CWT$_7$ represents the system when using (n-sym 5,7 with q-sh 16 filters) and OFDM DT-CWT$_8$ is the system when using (leg 5,3 with q-sh 18 filters).
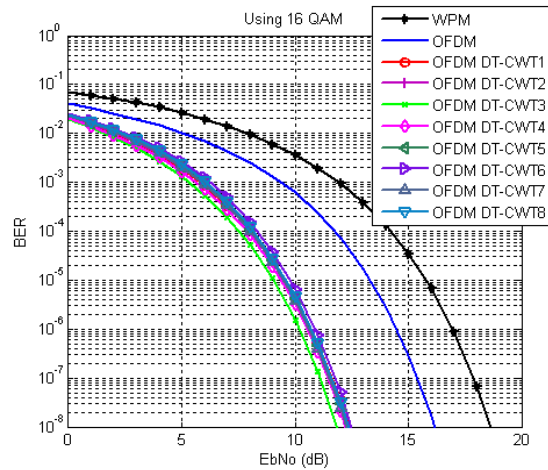

**Figure 5:** BER in 16QAM OFDM based on DT-CWT using different type of filters.
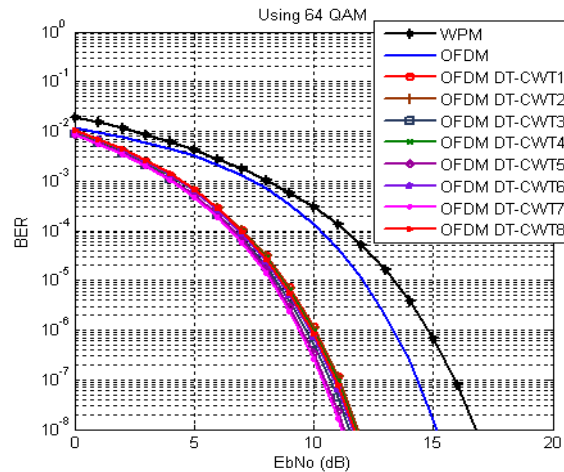
Figure 6: BER in 64QAM OFDM based on DT-CWT using different type of filters.

The results in fig. 5 (using 61 QAM) and fig. 6 (using 64 QAM) show that there is no degradation in the performance of the proposed system as a result of using different set of mismatching filters.

Next, the PAPR value of the proposed system is investigated and compared with the conventional OFDM and WPM systems in term of the complementary cumulative distribution function (CCDF).

In order to analyze PAPR, we generate the transmitted waveforms using 16 QAM modulation with 64 subcarriers and investigate the PAPR values for each of the three considered systems. Fig. 7 shows, the dynamic range of the PAPR signals of the three systems over a span of time. It is

quite clear that the proposed system is showing better performance than the conventional OFDM and WPM systems in terms of the range of variations of PAPR.
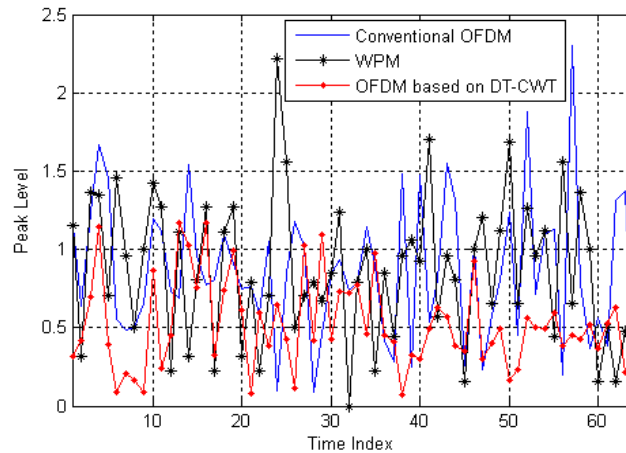
FIGURE 7: The Envelope of the Conventional OFDM, WPM and OFDM based on DT-CWT.

To quantify the PAPR values of the considered systems, the CCDF is obtained for each system. 16 QAM modulation scheme is used with 64 carriers. The results are shown in Figure 8. The figure shows that the DT-CWT based OFDM system achieves nearly 3 dB improvement over the conventional OFDM and WPM systems at 0.1% of CCDF.
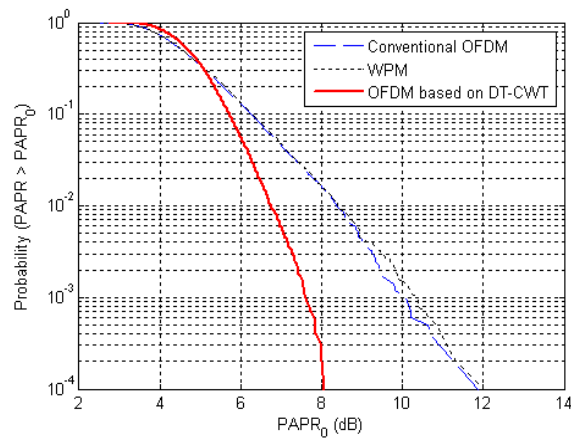
FIGURE 8: CCDF the Conventional OFDM, WPM and OFDM based on DT-CWT.

Next, the above experiment is repeated with the different set of filters as in the first experiment (16 QAM modulation scheme is used with 64 carriers). The results are shown in Figure 9.

Mohamed Nerma, Nidal Kamel, and Varun Jeoti
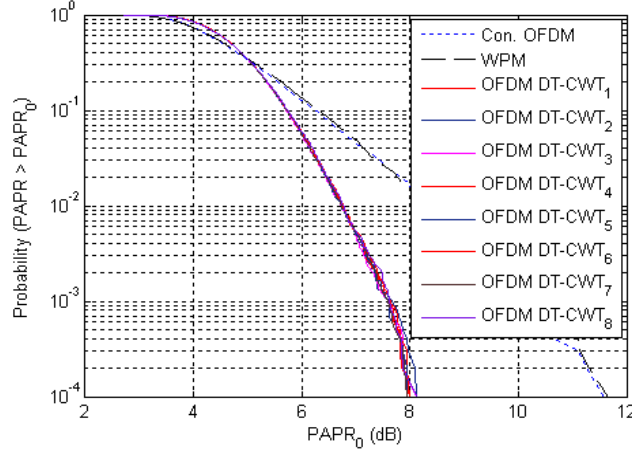
FIGURE 9: The effect of using different set of filters in design of the OFDM based on DT-CWT.

The results in fig. 9 show that there is no observed degradation in the performance of the DT-CWT based OFDM system as a result of using different set of mismatching filters.

In the third part of this experiment, the above experiments are repeated for conventional OFDM and OFDM based on (DT-CWT) systems using 16 QAM with different numbers of subcarriers (64, 128, 256, 512, and 1024). The results are shown in Figure 10 and Figure 11 respectively.
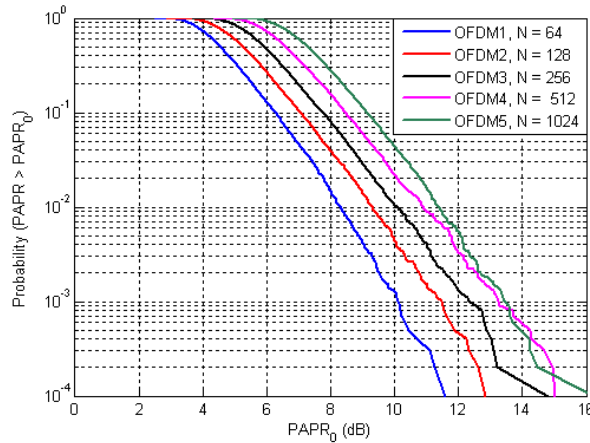
FIGURE 10: CCDF of PAPR for 16-QAM modulated conventional OFDM symbol with various values of subcarriers (N).

Theoretically, If $E\{|x[n]^2|\}$ is normalized to unity, then the CCDF of the PAPR is given by:

$$Pr[\lambda > \lambda_0] = 1 - \left(1 - e^{\left(-\frac{\lambda_0}{\sigma^2}\right)}\right)^N \qquad 23$$

Where N is the number of subcarriers.
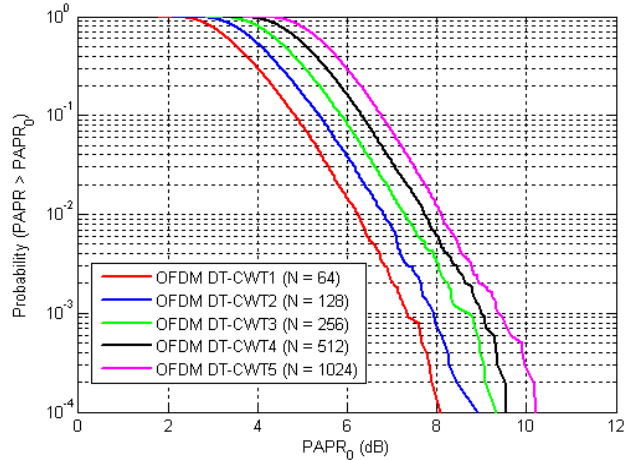
FIGURE 11: CCDF of PAPR for 16-QAM modulated OFDM based on DT-CWT symbol
with various values of subcarriers (*N*).

It is quite clear from Fig. 10 and Fig. 11 that the PAPR increases with the number of the subcarriers (see equation 23), and this is shared property between the proposed and the conventional OFDM systems. But, as the figures indicate the proposed system is showing better robustness towards PAPR performance degradation with increased number of subcarriers, than the conventional OFDM.

In the third experiment we test the spectrum of the three systems in terms of their power spectrum density. The results are shown in Figure 12.
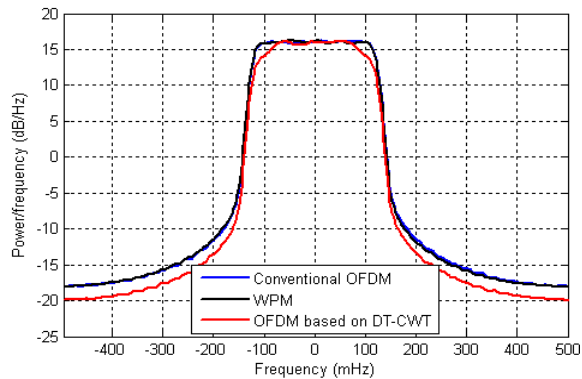
FIGURE 12: PSD of the Conventional OFDM, WPM and OFDM based on DT-CWT.

Figure 12 shows that, the proposed system is relatively showing better spectrum characteristics, in terms of more low out of band attenuation, than the conventional OFDM and the WPM systems.

Mohamed Nerma, Nidal Kamel, and Varun Jeoti

5. Conclusion

In this paper a new OFDM system based on DT-CWT is proposed. The performance of the proposed OFDM system is compared with the conventional OFDM and the WPM, in terms of BER and PAPR. The results show better BER performance by the proposed system to the conventional OFDM and the WPT and better performance by the conventional OFDM to the WPT. of BER than WPM system. In term of PAPR, the proposed system is showing significantly better performance (≈ 3dB) to the conventional OFDM and WPT. The results also show that there is no observed BER and PAPR degradation as a result of using different set of mismatching filters with the proposed DT-CWT based system.

REFERENCES

1. A. Jamin, and P. Mahonen, "Wavelet Packet Modulation for Wireless Communications", Wiley Wireless Communications and networking, Journal, vol. 5, no. 2, pp. 123-137, Mar. 2005.

2. M. K. Lakshmanan and H. Nikookar, "A Review of Wavelets for Digital Wireless Communication", Wireless Personal Communications Springer, 37: 387-420, Jan. 2006.

3. M. Guatier, J. Lienard, and M. Arndt, "Efficient Wavelet Packet Modulation for Wireless Communication", AICT'07 IEEE Computer Society, 2007.

4. I. W. Selesnick, "the Double Density Dual-Tree DWT", IEEE Transactions on Signal Processing, 52(5): 1304 – 1315, May 2004.

5. J. M. Lina,"Complex Daubechies Wavelets: Filter Design and Applications", ISAAC Conference, June 1997.

6. A. R. Lindsey and J. C. Dill, "Wavelet packet modulation: a generalized method for orthogonally multiplexed communications," in IEEE 27th Southeastern Symposium on System Theory, 1995, pp. 392–396.

7. A. R. Lindsey, "Wavelet packet modulation for orthogonally multiplexed communication," IEEE Transaction on Signal Processing, vol. 45, no. 5, pp. 1336–1339, May 1997.

8. C. V. Bouwel, J. Potemans, S. schepers, B. Nauwelaers, and A. Van Caelle, "wavelet packet Based Multicarrier Modulation", IEEE Communication and Vehicular Technology, SCVT 2000, pp. 131-138, 2000.

9. Ivan W. Selesnick, Richard G. Baraniuk, and Nick G. Kingsbury, "The Dual-Tree Complex Wavelet Transform," IEEE Signal Processing Mag, pp. 1053-5888, Nov 2005.

10. N.G. Kingsbury, "The dual-tree complex wavelet transform: A new technique for shift invariance and directional filters," in Proc. 8th IEEE DSP Workshop, Utah, Aug. 9–12, 1998, paper no. 86.

11. N.G. Kingsbury, "Image processing with complex wavelets," Philos. Trans. R. Soc. London A, Math. Phys. Sci., vol. 357, no. 1760, pp. 2543–2560, Sept. 1999.

12. N.G. Kingsbury, "A dual-tree complex wavelet transform with improved orthogonality and symmetry properties," in Proc. IEEE Int. Conf. Image Processing, Vancouver, BC, Canada, Sept. 10–13, 2000, vol. 2, pp. 375–378.

Mohamed Nerma, Nidal Kamel, and Varun Jeoti

13. N.G. Kingsbury, "Complex wavelets for shift invariant analysis and filtering of signals," Appl. Comput. Harmon. Anal., vol. 10, no. 3, pp. 234–253, May 2001.

14. I W. Selenick, "Hilbert transform pairs of wavelet bases," IEEE Signal Processing Lett., vol. 8, no. 6, pp. 170-173, June 2001.

15. H. Ozkaramanli and R. Yu, "on the phase condition and its solution for Hilbert transform pairs of wavelet bases," IEEE Trans. Signal Processing, vol. 51, no. 12, pp. 2393–3294, Dec. 2003.

16. R. Yu and H. Ozkaramanli, "Hilbert transform pairs of orthogonal wavelet bases: Necessary and sufficient conditions", IEEE Trans. Signal Processing IEEE Transactions on Signal Processing, vol. 53, no. 12, Dec. 2005.

17. R. Yu and H. Ozkaramanli, "Hilbert transform pairs of biorthogonal wavelet bases", IEEE Transactions on Signal Processing, VOL. 54, NO. 6, JUNE 2006.

18. I. W. Selesnick, "the Double Density Dual-Tree DWT", IEEE Transactions on Signal Processing, 52(5): 1304 – 1315, May 2004.

19. J. M. Lina,"Complex Daubechies Wavelets: Filter Design and Applications", ISAAC Conference, June 1997.

20. M. K. Lakshmanan and H. Nikookar, "A Review of Wavelets for Digital Wireless Communication", Wireless Personal Communications Springer, 37: 387-420, Jan. 2006.

21. R. Van Nee and A. De Wild, "reduction the peak-to average power ratio of OFDM" 48th IEEE Vehicular Technology Conference, Ottawa, Canada, May 18-21, 1998; 2072-2076, IEEE New York, USA.

22. H. Ochiai and H. Imai, "On the disitribution of the peak-to-average power ratio in OFDM signals", IEEE Trans. Commun. 2001; 49, 282-289.

23. S. wei, D. L. Goeckel, and P. E. Kelly "A modern extreme value theory approach to calculate the distribution of the peak-to-average power ratio in OFDM systems", IEEE International Conference on Communications, New York, Apr. 28- May 2, 2002; vol. 3, 1686-1690; IEEE New York, USA.

24. H. Yu, M. Chen and G. wei "Distribution of PAPR in DMT systems", Electron. Lett. 2003; 39, 799-801.

25. R. Rajbanshi, A. M. Wyglinski and G. J. Minden, "Multicarrier Transceivers: Peak-to-average power ratio reduction", IEEE Commun. Society. WCNC 2008 proceedings.

Mohamed Hussien Mohamed Nerma was born in Khartoum, Sudan. He received the B.Sc. degree in Electrical Engineering (Control) from Sudan University of Science and Technology (SUST), Sudan in 1999. He received the M.Sc. degree in Communication Engineering from Karary Academy of Technology, Sudan in 2002. From 2002 to 2006 he was lecturer in the Sudan University of Science and Technology. He is currently PhD. Student in University Technology PETRONAS, Malaysia.

Mohamed Nerma, Nidal Kamel, and Varun Jeoti

Nidal S. Kamel received his Ph.D degree (Hons) in telecommunication and statistical signal processing from the Technical University of Gdansk, Poland, in 1993. His research is focused on linear estimation, noise reduction, pattern recognition, optimal filtering, and telecommunications. Currently he is working for Universiti Teknologi PETRONAS, Malaysia. He is senior member of IEEE.

Varun Jeoti Jagadish received his Ph.D. degree from Indian Institute of Technology Delhi India in 1992. He worked on several sponsored R&D projects in IIT Delhi and IIT Madras during 1980 to 1989 developing Surface Acoustic Wave Pulse Compression filters, underwater optical receivers etc.. He was a Visiting Faculty in Electronics department in Madras Institute of Technology for about 1 year during 1989 to 1990 and joined Delhi Institute of Technology for next 5 years till 1995. He moved to Electrical & Electronic Engineering (E&E Engg) department of Universiti Sains Malaysia in 1995 and joined E&E Engg of Universiti Teknologi PETRONAS in 2001. His research interests are in Wireless LAN and MAN technologies, DSL technology and related signal processing.

Dwpt Based FFT and ITS Application to SNR Estimation in OFDM Systems

Rana Shahid Manzoor   engr.shahid@gmail.com
Regina Gani   reginagani@gmail.com
Varun Jeoti   varun_jeoti@petronas.com.my
Nidal Kamel   nidalkamel@petronas.com.my
Muhammad Asif   asf_kh@yahoo.com

Electrical & Electronic Engineering Department,
Universiti Teknologi PETRONAS (UTP),
Bandar Seri Iskandar, Tronoh, 31750, Malaysia

ABSTRACT

In this paper, wavelet packet (WP) based FFT and its application to SNR estimation is proposed. OFDM systems demodulate data using FFT. The proposed solution computes the exact FFT using WP and its computational complexity is of the same order as FFT, i.e. $O(N \log_2 N)$. SNR estimation is done inside wavelet packet based FFT block unlike other SNR estimators which perform SNR estimation after FFT. The data, so analyzed using wavelet packets, is used to perform SNR estimation in colored noise. The proposed estimator takes into consideration the different noise power levels of the colored noise over the OFDM sub-carriers. The OFDM band is divided into several sub-bands using wavelet packet and noise in each sub-band is considered white. The second-order statistics of the transmitted OFDM preamble are calculated in each sub-band and the power of the noise is estimated. The proposed estimator is compared with Reddy's estimator for colored noise in terms of mean squared error (MSE).

Keywords: SNR, Noise power estimation, Wavelet Packet, Adaptive modulation, OFDM.

---

1. INTRODUCTION

Fourth Generation wireless and mobile systems characterized by broadband wireless systems are currently the focus of research and development among the researchers everywhere. The broadband wireless systems favor the use of orthogonal frequency division multiplexing (OFDM) modulation that allows high data-rate communication. A major advantage of OFDM systems is its ability to divide the input high rate data stream into many low-rate streams that are transmitted in parallel. Doing so increases the symbol duration and reduces the intersymbol interference over

frequency-selective fading channels. This and other features of equivalent importance have motivated the adoption of OFDM as a standard for several applications such as digital video broadcasting (DVB) and broadband indoor wireless local area networks, broadband wireless metropolitan area networks and many others.

In order to exploit all these advantages and maximize the performance of OFDM systems; channel state information (CSI) plays a very important role. Signal-to-noise ratio (SNR) is a quantity that gives a comprehensive measure of CSI for each frame. An on-line SNR estimator thus provides the knowledge to decide whether a transition to higher bit rates would be favorable or not.

Signal-to-noise ratio (SNR) is defined as the ratio of the desired signal power to the noise power. Noise variance, and hence, SNR estimates of the received signal are very important parameters for the channel quality control in communication systems [1]. The search for a good SNR estimation technique is motivated by the fact that various algorithms require knowledge of the SNR for optimal performance. For instance, in OFDM systems, SNR estimation is used for power control, adaptive coding and modulation, turbo decoding etc.

SNR estimation indicates the reliability of the link between the transmitter and receiver. In adaptive system, SNR estimation is commonly used for measuring the quality of the channel and accordingly changing the system parameters. For example, if the measured channel quality is low, the transmitter may add some redundancy or complexity to the information bits (more powerful coding), or reduce the modulation level (better Euclidean distance), or increase the spreading rate (longer spreading code) for lower data rate transmission. Therefore, instead of implementing fixed information rate for all levels of channel quality, variable rates of information transfer can be used to maximize system resource utilization with high quality of user experience [2].

Many SNR estimation algorithms have been suggested in the last ten years [1]-[6] and also successfully implemented in OFDM systems using the pilot symbols [1,2,5]. Extracting pilots and using them for SNR estimation is computationally complex. The essential requirement for an SNR estimator in OFDM system is of low computational load. This is in order to minimize hardware complexity as well as the computational time. This is the motivating factor for the pursuit of an SNR estimator that does not require the manipulation of pilot symbols. SNR estimator, presented in the past, performed SNR estimation using pilot symbols at the back-end of the receiver in the OFDM system [2]. The SNR estimator presented in this paper performs SNR estimation inside FFT and makes use of only one OFDM synchronization preamble. In many SNR estimation techniques, noise is assumed to be uncorrelated or white. But, in wireless communication systems, where noise is mainly caused by a strong interferer, noise is colored in nature. According to best knowledge of authors, so far only Reddy's estimator considered colored noise scenario. Hence we use his work for the purpose of comparison in this paper. Reddy's estimator makes use of several OFDM symbols to perform SNR estimation; hence the computational complexity of finding good estimates is very high. So there is enough interest to design an efficient SNR estimator that is computationally simple.

OFDM demodulation uses discrete Fourier transform (DFT). An FFT (fast Fourier transform) is used to demodulate data. In this paper a novel wavelet packet based FFT and its application to SNR estimation is presented. The proposed solution computes the exact result, and its computational complexity is same order of FFT, i.e. $O(Nlog_2 N)$.

The proposed SNR technique performs SNR estimation inside FFT unlike previous SNR estimators. SNR estimator for the colored noise in OFDM system is proposed. The algorithm is based on the two identical halves property of time synchronization preamble used in some OFDM systems. The OFDM band is divided into several sub-bands using wavelet packet and noise in each sub-band is considered white. The second-order statistics of the transmitted OFDM preamble are calculated in each sub-band and the power noise is estimated. Therefore, the

Rana Shahid Manzoor, Regina Gani, Varun Jeoti, Nidal Kamel & Muhammad Asif

proposed approach estimates both local (within smaller sets of subcarriers) and global (over all sub-carriers) SNR values. The short term local estimates calculate the noise power variation across OFDM sub-carriers. When the noise is white, the proposed algorithm works as good as the conventional noise power estimation schemes, showing the generality of the proposed method.

The remainder of the paper is organized as follows. In Section 2, the proposed wavelet packet based FFT technique is presented. Section 3 provides the proposed SNR estimation. Section 4 describes the Reddy' SNR estimator used for comparison with proposed SNR estimator. Section 5 presents simulation results and discussion. Section 6 concludes the paper.

2. PROPOSED WAVELET PACKET BASED FFT (DWPT-FFT)

The fundamental principle that the FFT relies on is that of decomposing the computation of the discrete Fourier transform of a sequence of length N into successively smaller discrete Fourier transforms of the even and odd parts. In the proposed method the even – odd separation is replaced by wavelet packet decomposition.

The block diagram of proposed DWPT-FFT is shown in Figure 1. The idea is borrowed from Guo [7]. Wavelet packet based FFT first performs Wavelet Packet decomposition, followed by reduced size FFT and butterfly operation as shown in Figure1. This can be extended so that WP analysis is 3 to 4 level analysis and FFT is $N/4$, $N/8$ or $N/16$ size FFT. Butterfly is appropriately designed.
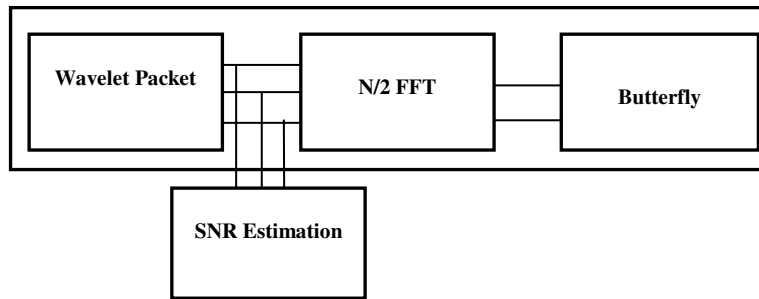

Figure 1: Block diagram of DWPT-FFT

The wavelet packet based FFT (DWPT-FFT) is represented by equation 1:

$$F_N = \begin{bmatrix} A_{N/2} & B_{N/2} \\ C_{N/2} & D_{N/2} \end{bmatrix} \begin{bmatrix} F_{N/2} & 0 \\ 0 & F_{N/2} \end{bmatrix} \begin{bmatrix} WP_N \end{bmatrix} \tag{1}$$

where $A_{N/2}, B_{N/2}, C_{N/2}$ and $D_{N/2}$ are all diagonal matrices. In equation 1, the values on the diagonal of $A_{N/2}$ and $C_{N/2}$ are the length-N DFT of 'h', the scaling filter coefficients, and the values on the diagonal of $B_{N/2}$ and $D_{N/2}$ are the length-N DFT of 'g', the wavelet filter coefficients. The factorization can be visualized as
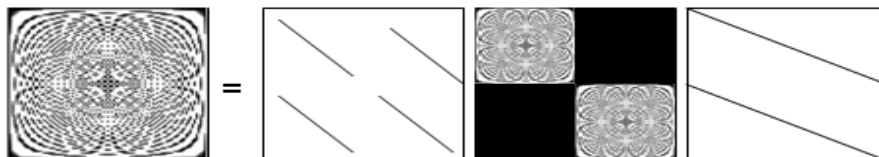
where we image the real part of DFT matrices, and the magnitude of the matrices for butterfly operations and the one-scale DWPT using *db3* wavelets. Clearly we can see that the twiddle factors have non-unit magnitude.

The above factorization suggests a DWPT-FFT algorithm. The block Diagram of length 8 algorithm is shown in Figure 2. Following this, the high pass and the low pass DWPT outputs go through separate length-4 DFT, then they are combined with butterfly operations.

Same procedure in Figure2 is iteratively applied to short length DFTs to get the full DWPT based FFT algorithm where the twiddle factors are the frequency wavelet filters. The detail of butterfly operations is shown in Figure 3 where '*i*' belongs to {*0,1,....N/2-1*}.
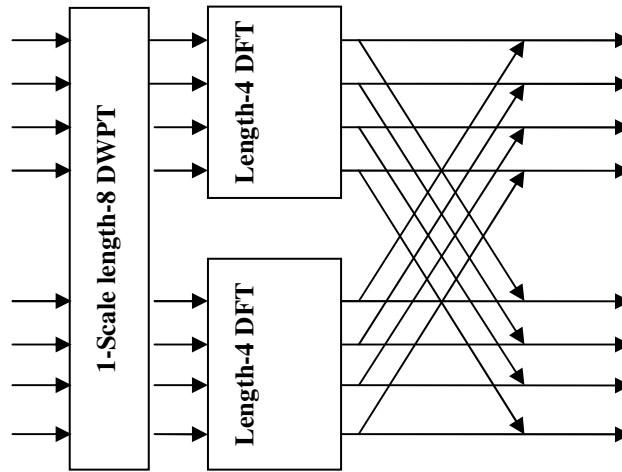


Figure 2: Last stage of length 8 DWPT-FFT
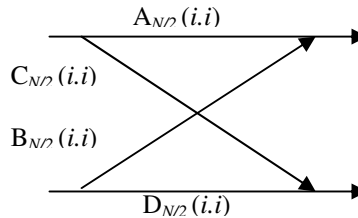
**Figure 3:** Butterfly operation in DWPT-FFT
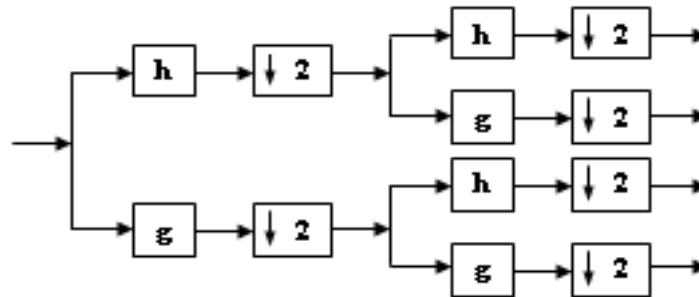
Figure 4: Two-scale discrete wavelet packet transforms

Wavelet packet allows a finer and adjustable resolution of frequencies at high frequency. Input data are first filtered by pair of filters **h** and **g** (low pass and high pass respectively) and then down sampled. The same analysis is further iterated on both low and high frequency bands as shown in Figure 4.

For the DWPT based FFT algorithm, the computational complexity is also $O\ (N\ log2N)$. However, the constant appears before $N\ log_2 N$ depends on the wavelet filters used.

3. SNR ESTIMATION

Wavelet Packet analyzed data becomes available for SNR estimation inside FFT block as shown in figure1. The synchronization OFDM preamble - the preamble which has two identical halves property as shown in figure 5, is obtained by loading constellation points with a PN sequence (P_{seq}) at even sub-carriers using equation 2 [9]:

$$P_{even}(k) = \begin{cases} \sqrt{2} . P_{seq}(k) & k=2m \\ 0 & k=2m+1 \end{cases} \qquad m=1,2,3....n \qquad (2)$$

where the factor of $\sqrt{2}$ is related to the 3 dB boost and 'k' shows the sub-carriers index. OFDM training/synchronization data of length 'N' is sent from the transmitter (T_x). To avoid intersymbol interference (ISI), a cyclic prefix (CP) is added.

After removing cyclic prefix at receiver, OFDM data is divided into 2^n sub-bands using periodic wavelet packets where 'n' shows the number of levels. The length of each sub-band is $N_{sub} = N/2^n$. It inherits the two identical halves property of synchronization preamble. The noise in each sub-band is considered white. The system's parameters and the structure of wavelet packet used for the simulations are calculated using [9] as shown in table 1.
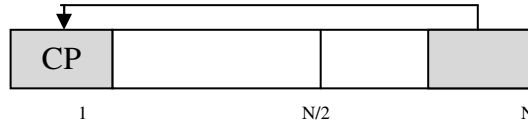
Figure 5: OFDM training symbol with cyclic prefix.

3.1. SIGNAL POWER AND NOISE POWER ESTIMATION

The received signal in the kth sub band is $r_k(n)$ and it is expressed as,

$$r_k(n) = s_k'(n) + n_k(n)$$
$$= s_k(n) * h_k(n) + n_k(n) \qquad (3)$$

The autocorrelation function of the received signal in k_{th} sub-band, $R^k_{rr}(m)$ has the following relationship to the autocorrelation of the transmitted sub-band signal, $R^k_{s's'}(m)$ and the noise, $R^k_{nn}(m)$:

$$R^k_{rr}(m) = R^k_{s's'}(m) + R^k_{nn}(m) \qquad (4)$$

Rana Shahid Manzoor, Regina Gani, Varun Jeoti, Nidal Kamel & Muhammad Asif

where $R_{s's'}^{k}(m) = \alpha_k R_{ss}(m)$, α_k is the attenuated channel power in the kth sub-band. Over a small bandwidth of kth sub band, it is safe to assume that, even in frequency selective channels, the attenuation is constant and equal to α_k .

The noise in channel is modeled as additive white Gaussian noise, thus its autocorrelation function can be expressed as

$$R_{nn}(m) = \sigma^2 \delta(m) \tag{5}$$

where δ (m) is the discreet delta sequence and σ^2 is the power of noise.

A study of the OFDM signal shows that, as all the sub-carriers are present with equal power over the signal bandwidth, the power spectrum of an OFDM signal is nearly white and hence its autocorrelation is also given by

$$R_{s's'}(m) = \alpha_k \delta(m) \tag{6}$$

Hence, at zero lag, the autocorrelation contains both the signal power estimate and noise power estimate indistinguishable from each other.

However, because of the identical halves nature of the preamble the autocorrelation also has peaks where one half matches with other half on both sides of the zero delay. The autocorrelation of the transmitted and received scale 5 sub-band signal at SNR = 7 dB are shown in figure 6(a) and figure 6(b), respectively. It is clear that the autocorrelation values apart from the zero-offset are unaffected by the AWGN, so one can find the signal and noise powers from the zero-lag autocorrelation value 'L'.

Taking into consideration the autocorrelation values for $L-N_{sub}/2$ and $L+N_{sub}/2$ signal power is given as

$$\hat{\alpha} = 2R_{rr}(L - N_{sub}/2) \tag{7}$$

Or

$$\hat{\alpha} = 2R_{rr}(L + N_{sub}/2) \tag{8}$$

Having obtained the power of signal in certain sub-band, noise power can be calculated using equation 8.

$$\hat{\sigma}^2 = R_{rr}(L_{sub}) - \hat{\alpha} \tag{9}$$

Finally we can find the SNR estimates in the sub-band by using equation (7 or 8) and equation (9):

$$S\hat{N}R = \frac{\hat{\alpha}}{\hat{\sigma}^2} \tag{10}$$

where $S\hat{N}R$ is the estimated value for SNR.
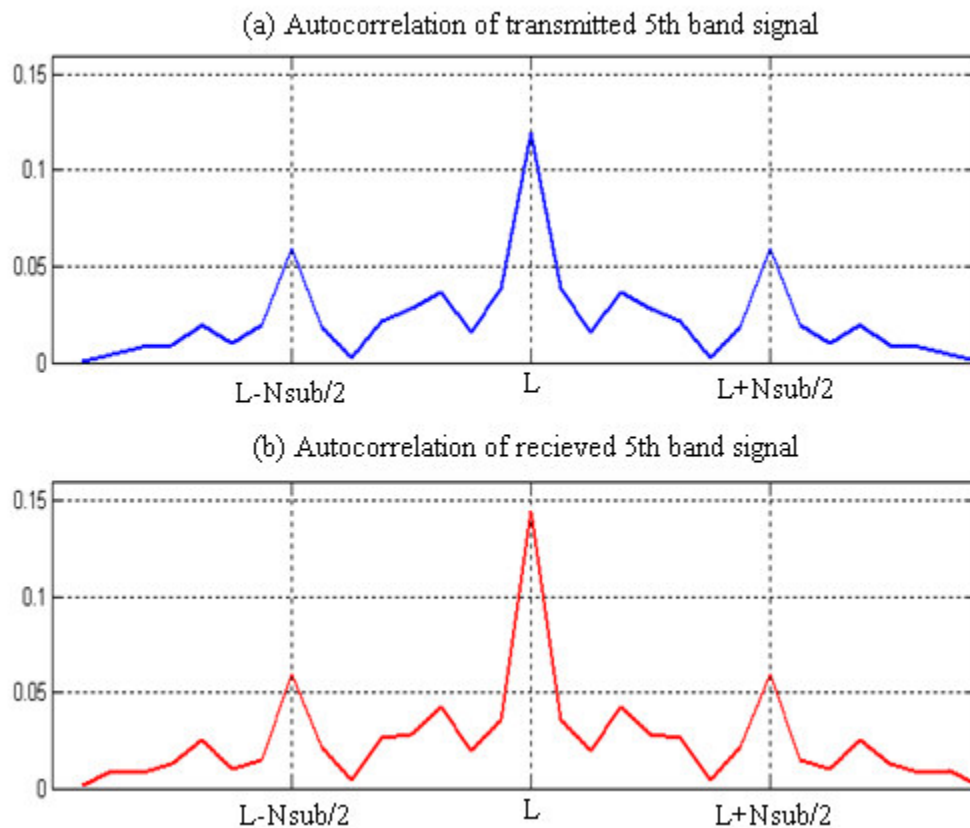
Figure 6: Autocorrelation plot of transmitted (a) and received (b) 5th band signal

4. REDDY'S SNR ESTIMATOR FOR COLORED NOISE

In this method channel estimation is performed in the first realization of the channel, using pilot symbols and this estimate is used to estimate the signal noise power. The suggested method can be used Additive White Gaussian Noise (AWGN) channel and for color dominated channel, in which the noise power varies across the frequency spectrum [2].

The system model is described in the frequency domain, where a signal is transmitted to obtain the estimated channel frequency response after which the instantaneous noise power mean square is determined. The transmitted signal includes white noise which is added by the channel of unknown amplitude. This is modeled in the frequency domain by the equation:

$$R_m(k) = S_m(k)H_m(k) + N_m(k) \qquad (11)$$

where

$S_m(k)$ = Transmitted signal

$R_m(k)$ = Received signal

$N_m(k)$ = Channel white noise

The channel frequency response is estimated by transmitting preamble and performing division in the frequency domain of the received signal by the transmitted signal. When performing the division, the effect of noise is ignored. The pilot symbols are then used as the transmitted signal and the received signal in the pilot sub-carriers is used for the received signal and the estimated transfer function inserted in the equation to determine the noise power estimate. The noise power estimation is found by finding the difference between the noisy received signal and the noiseless signal.

$$\sigma^2{}_m(k) = \left| R_m(k) - \hat{S}_m(k)\hat{H}_m(k) \right|^2 \tag{12}$$

The difference between the actual channel frequency response and the estimated is the channel estimation error.

5. RESULTS AND DISCUSSIONS

In this section, we will first show that DWPT based FFT algorithm is able to compute FFT exactly. Following that, we will present the performance results of proposed estimator designed using wavelet packet based FFT. The results would include mean squared error of our estimation as compared to that of Reddy's.

The proposed DWPT-FFT computes the exact result. In order to show that the example of a chirp signal is taken and its FFT computed both from DWPT based algorithm and discrete Fourier transform (DFT) equation. The chirp signal is defined by $x(n) = e^{j\pi n^2}/N$, and its FFT as computed using DWPT and DFT are shown in figure 7.
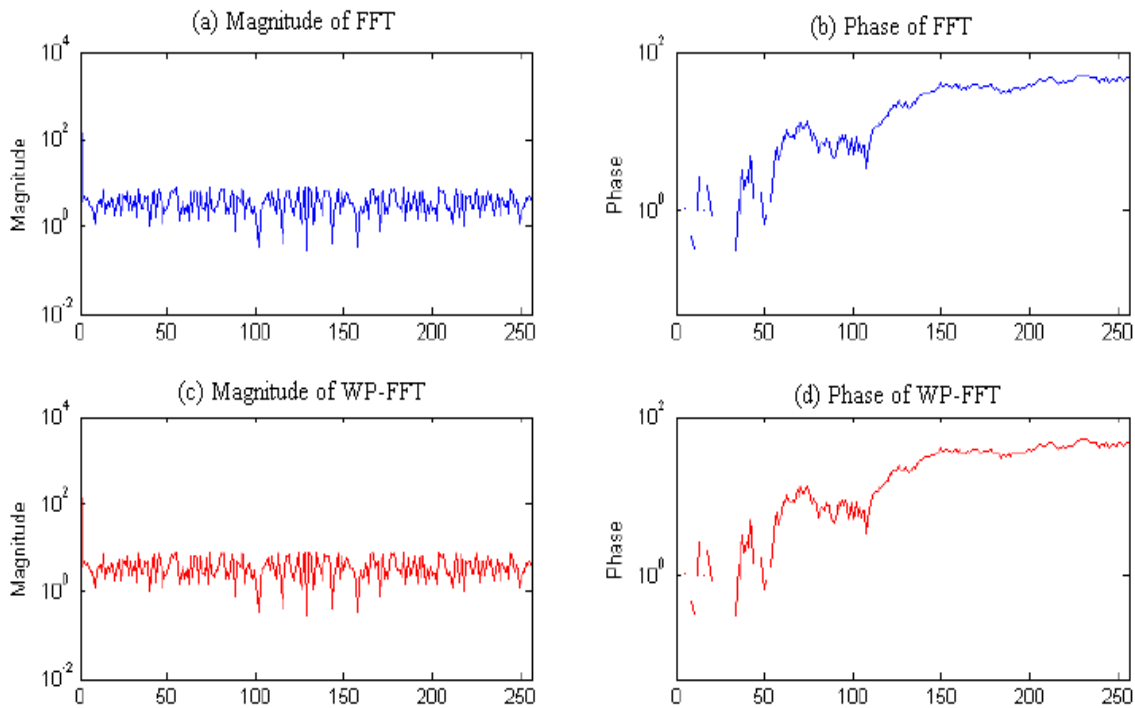

Figure 7: FFT result with and without wavelet packet

This performance of our estimator is measured in terms of Mean Squared Error. To obtain these results, OFDM system parameters given in Table 1 were chosen. The proposed SNR estimator is compared with Reddy's estimator for colored noise in OFDM systems. The parameters given in Table 1 are same for both estimators except that for Reddy's estimator 50 OFDM symbols are used to perform SNR estimation.

SNR is varied from 1 dB to 14 *dB* for each sub-band and the mean-squared error (MSE) is derived for the estimated SNR from 2000 trials according to the following formula

$$MSE = \frac{1}{2000} \sum_{i=1}^{2000} (S\hat{N}R(i) - SNR)^2 \qquad (13)$$

From figure 8 and figure 9 it is clear that the proposed estimator gives better performance in SNR estimation as compared to Reddy estimator. It is observed that the proposed technique can estimate local statistics of the noise power when the noise is colored.

Table 1: Parameters for the simulation

Ifft size	256
Sampling Frequency = F_s	20*MHz.*
Sub Carrier Spacing= $\Delta f = F_s/Ifft$	1×10^5
Useful Symbol Time = $T_b = 1/\Delta f$	1×10^{-5}
CP Time $= T_g = G * T_b$ *where* $G = 1/4$	2.5×10^{-6}
OFDM Symbol Time $= T_s = T_b + T_g$	1.25×10^{-5}
$T_s = 5/4 * T_s$ *(Because ¼ CP makes the sampling faster by 5/4 time*	1.56×10^{-5}
$T_{sub} = T_s/16$	9.8×10^{-7}
Wavelet Packet Object Structure	
Wavelet Decomposition Command : wpdec *Size of initial data : [1 320]* *Order= 2* *Deptth=: 4* *Terminal nodes : [15 16 17 18 19 20 21 22* * 23 24 25 26 27 28 29 30]* *--* *Wavelet Name : Daubechies (db3) ,* *Entropy Name : Shannon*	
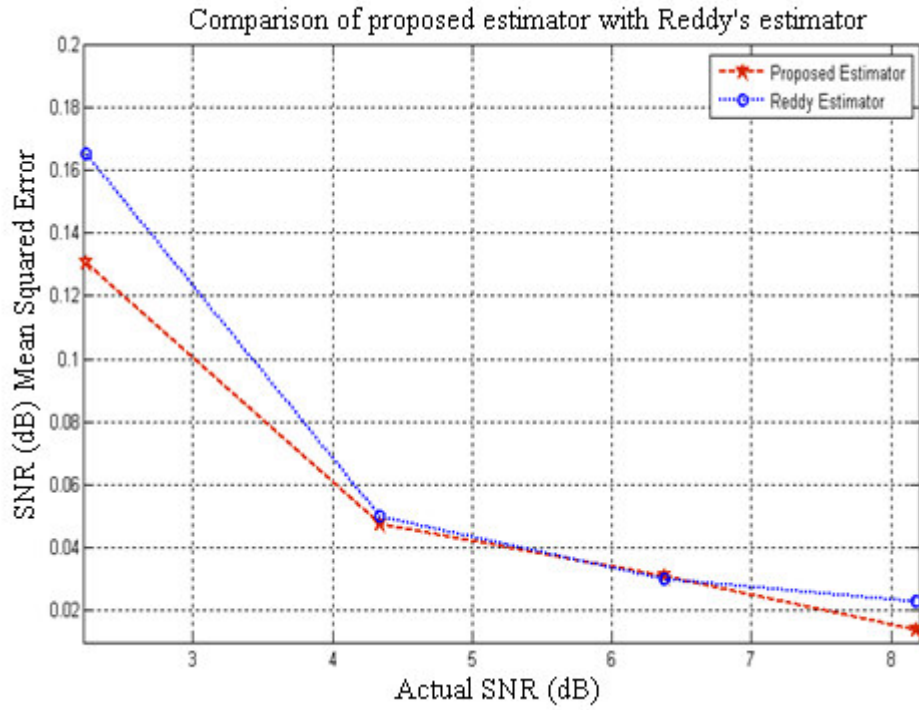
Figure 8: MSE performance of the proposed technique
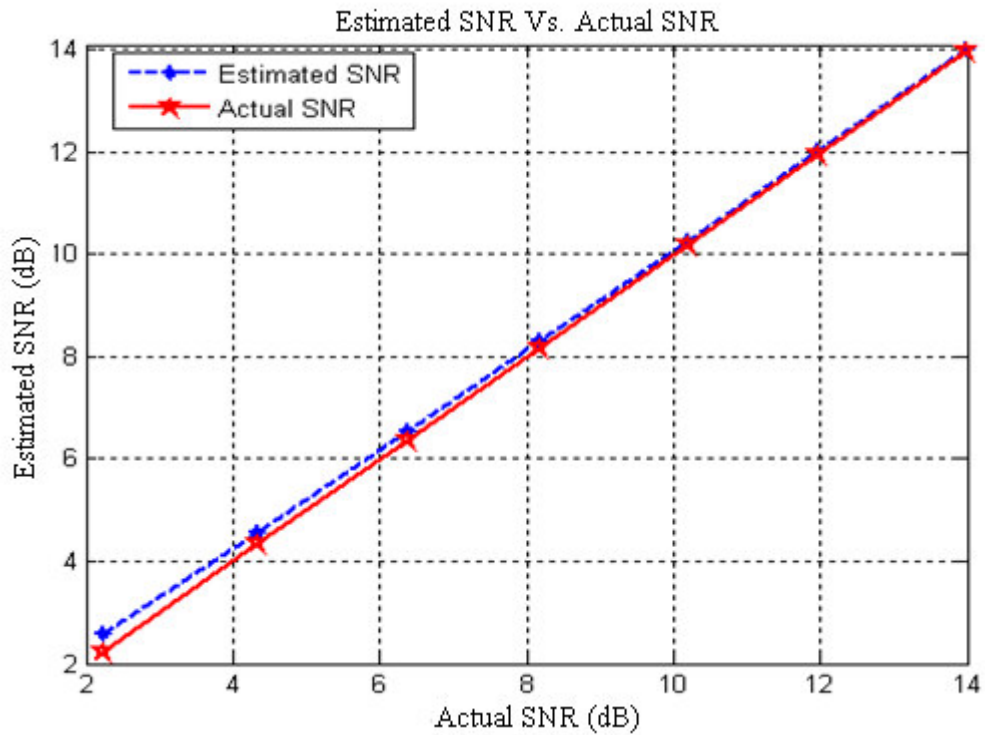
Figure 9: Actual SNR vs. Estimated SNR of colored noise

Rana Shahid Manzoor, Regina Gani, Varun Jeoti, Nidal Kamel & Muhammad Asif

Complexity of proposed technique:

The proposed wavelet packet based FFT computes the exact result, and its computational complexity is of the same order of FFT, i.e. $O(\log_2 N)$.

The proposed autocorrelation based SNR estimator inside FFT makes use of one OFDM preamble so its complexity is $\sim 2N^3$ as compared to Reddy' estimator which have complexity $\sim 50N^3$ (where 50 shows the number of OFDM symbols used to get better SNR estimates after averaging over these OFDM symbols). The proposed estimator has relatively low computational complexity because it makes use of only one OFDM preamble signal to find the SNR estimates. The proposed estimator fulfills the criteria of a good SNR estimator because it is unbiased (i.e. it exhibits the smallest bias) and has the least variance of SNR estimates as seen from mean squared error diagrams..

6. CONCLUSION

In this paper, an algorithm to compute FFT using discrete wavelet packets is developed and applied to the problem of SNR estimation in OFDM systems inside FFT. Also, the technique is extended to SNR estimation under colored noise where the variation of the noise power across OFDM sub-carriers is allowed. The second-order statistics of the transmitted OFDM preamble are calculated in each sub-band and the noise power is estimated. Therefore, the proposed approach estimates both local (within smaller sets of subcarriers) and global (over all sub-carriers) SNR values. The short term local estimates calculate the noise power variation across OFDM sub - carriers. The results show that the proposed estimator performs better than other conventional methods. Complexity to find SNR estimates is much lower because our estimator makes use of only one OFDM preamble signal. This estimator fulfills the criteria of a good SNR estimator as it is unbiased and has the smallest variance of SNR estimates.

REFERENCES

1. Xiaodong X., Ya Jing. and Xiaohu Y. "*Subspace- Based Noise Variance and SNR Estimation for OFDM Systems*", IEEE Wireless Communications and Networking Conference, 2005

2. Reddy, S. and Arslan H. "*Noise Power and SNR Estimation for OFDM Based Wireless Communication Systems",* Wireless Communication and Signal Processing Group, 2003

3. Kamel N.S. and Joeti V. "*Linear prediction based approach to SNR   estimation in AWGN channel*", 23rd Biennial Sympiosium on Communications,2006

4. Pauluzzi D.R. and Norman C.B. *"A Comparison of SNR Estimation techniques for the AWGN Channel*", IEEE Transactions on Communications, Vol. 48 no. 10, 2000

5. Bournard, S. "*Novel Noise Variance and SNR Estimation Algorithm for Wireless MIMO OFDM Systems*", IEEE GLOBECOM vol., 2003

6. Oppenheim, A. V.; Schafer, R. W.: "Discrete-Time Signal Processing",Prentice-Hall, 1989.

7. Guo, H.; Burrus, C. S.: "Wavelet Transform Based Fast Approximate Fourier Transform", Proc. of ICAASP-1997, Munich, Germany.

8. Prasad, R. "*OFDM for Wireless Communications Systems",* Boston, Artech House Inc., 2004

Rana Shahid Manzoor, Regina Gani, Varun Jeoti, Nidal Kamel & Muhammad Asif

9. IEEE 802.16-2004,"*IEEE Standard for Local and Metropolitan Area Networks Part 16: Air Interface for Fixed Broadband Wireless Access Systems",* 2004

10. IEEE 802.11a, 1999. "*Standard for local and metropolitan area networks: Wireless LAN Medium Access Control (MAC) and Physical Layer (PHY) specifications. High Speed Physical Layer in the 5 GHz Band".* New York: The Institute of Electrical and Electronics Engineers Inc., 1999.

11. IEEE802.11g, 2003. "*Standard for local and metropolitan area networks: Wireless LAN Medium Access Control (MAC) and Physical Layer (PHY) specifications – Amendment 4: Further Higher Data Rate Extension in the 2.4 GHz Band",* New York: The Institute of Electrical and Electronics Engineers Inc., 2003.

12. IEEE802.16, 2001. "*Standard for local and metropolitan area networks: Air interface for fixed broadband wireless access systems*" New York: The Institute of Electrical and Electronics Engineers Inc., 2001.

13. IEEE802.16a, 2003. "*Standard for local and metropolitan area networks: Air interface for fixed broadband wireless access systems – Amendment 2: Medium access control modifications and additional physical layer specifications for 2-11 GHz".* New York: The Institute of Electrical and Electronics Engineers Inc.,2003.

14. Jakes., 2004, "*Microwave Mobile Communications".* New York: Wiley, 2004.

15. Van Nee, 2000 "*OFDM for wireless multimedia communications*. London: Artech House.

16. H. Van Trees., 1968 "*Detection, Estimation, and Modulation Theory",* vol.1, New York, Wiley.

17. H. Hayes, 1996, Statistical *Digital Signal Processing and Modeling*, John Wiley.

18. Haykin, S. and Moher, M. "*Modern Wireless Communicatios*", Ontario, Pearson Education Inc., 2005

19. Haykin, 2005., "*Modern Wireless Communicatios*" Ontario, Pearson Education Inc.

20. Dr. Aditya Goel et, al. "Integrated Optical Wireless Network For Next Generation Wireless Systems", Signal Processing: An International Journal (SPIJ), Volume (3): Issue (1).